*Articles*

# Cholesterol Superlattice Modulates the Activity of Cholesterol Oxidase in Lipid Membranes†

Mei Mei Wang,‡ Michelle Olsher,‡ István P. Sugár,§ and Parkson Lee-Gau Chong*,‡

*Department of Biochemistry, Temple University School of Medicine, Philadelphia, Pennsylvania 19140, and Departments of Biomathematical Sciences and of Physiology and Biophysics, Mount Sinai Medical Center, New York, New York 10029*

*Received November 6, 2003; Revised Manuscript Received December 22, 2003*

ABSTRACT: Here, the interplay between membrane cholesterol lateral organization and the activity of membrane surface-acting enzymes was addressed using soil bacteria cholesterol oxidase (COD) as a model. Specifically, the effect of the membrane cholesterol mole fraction on the initial rate of cholesterol oxidation catalyzed by COD was investigated at 37 °C using cholesterol/1-palmitoyl-2-oleoyl-L-α-phosphatidylcholine (POPC) large unilamellar vesicles (LUVs, ∼800 nm in diameter). In the three concentration ranges examined (18.8−21.2, 23.6−26.3, and 32.2−34.5 mol % cholesterol), the initial activity of COD changed with cholesterol mole fraction in a biphasic manner, exhibiting a local maximum at 19.7, 25.0, and 33.4 mol %. Within the experimental errors, these mole fractions agree with the critical cholesterol mole fractions ($C_r$) (20.0, 25.0, and 33.3) theoretically predicted for maximal superlattice formation. The activity variation with cholesterol content was correlated well with the area of regular distribution ($A_{reg}$) in the plane of the membrane as determined by nystatin fluorescence. A similar biphasic change in COD activity was detected at the critical sterol mole fraction 20 mol % in dehydroergosterol (DHE)/POPC LUVs (∼168 nm in diameter). These results indicate that the activity of COD is regulated by the extent of sterol superlattice for both sterols (DHE and cholesterol) and for a wide range of vesicle sizes (∼168−800 nm). The present work on COD and the previous study on phospholipase $A_2$ ($sPLA_2$) [Liu and Chong (1999) *Biochemistry 38*, 3867−3873] suggest that the activities of some surface-acting enzymes may be regulated by the extent of sterol superlattice in the membrane in a substrate-dependent manner. When the substrate is a sterol, as it is with COD, the enzyme activity reaches a local maximum at $C_r$. When phospholipid is the substrate, the minimum activity is at $C_r$, as is the case with $sPLA_2$. Both phenomena are in accordance with the sterol superlattice model and manifest the functional importance of membrane cholesterol content.

Regulation of membrane surface-acting enzymes is an important issue in lipid metabolism and signal transduction (*1*−*5*). Many studies show that membrane physical properties play a crucial role in the activities of surface-acting enzymes (*6*−*8*). However, how the membrane lateral organization of cholesterol, a major component in mammalian cell membranes, affects surface-acting enzymes remains elusive.

In this study, the interplay between membrane cholesterol lateral organization and the activities of membrane surface acting enzymes was addressed using soil bacteria cholesterol oxidase (COD)[1] (3-β-hydroxysteroid oxidase, EC 1.1.3.6, ∼55 kDa) as a model. COD is a water-soluble, flavin adenine dinucleotide-containing enzyme, which catalyzes the oxidation of cholesterol (the rate-limiting step) and the isomerization of cholest-5-en-3-one into cholest-4-en-3-one (Scheme 1) (*9*, *10*). This enzymatic reaction has been applied clinically to determine the total serum cholesterol level for assessment of the risk of coronary heart disease and other lipid disorders. The amino acid and nucleotide sequence (*11*−*13*) and X-ray crystal structures of COD from soil bacteria *Brevibacterium sterolicum* and *Streptomyces hygroscopicus* in the absence and presence of substrate (*14*−*16*) have been reported. One current paradigm for how COD works in membrane systems is as follows. It first binds to the surface of the lipid bilayer with little membrane disruption (*14*, *15*, *17*). Then, COD undergoes a conformational change, forming a lid with a

† This work was supported by grants from the American Heart Association (9950320N and 0255082N). Acknowledgment is also made to the donors of the American Chemical Society Petroleum Research Fund for partial support of this research (PRF 38205-AC7). M.O. was a recipient of federal work-study awards and a Temple University fellowship. I.P.S. is grateful for Mrs. Lawrence Garner's generous support and for a grant from Pfizer Inc.

* To whom correspondence should be addressed. Phone: 215-707-4182. Fax: 215-707-7536. E-mail: pchong02@temple.edu.

‡ Temple University School of Medicine.

§ Mount Sinai Medical Center.

[1] Abbreviations: $A_{reg}$, the area of regular distribution in the plane of the membrane; COD, cholesterol oxidase; $C_a$, sterol mole fractions for maximal COD activity; $C_p$, sterol mole fractions for maximal $A_{reg}$; $C_r$, theoretically predicted critical sterol mole fractions for maximal superlattice formation; DHE, dehydroergosterol; DMPC, dimyristoyl-L-α-phosphatidylcholine; LUV, large unilamellar vesicles; MLV, multilamellar vesicles; POPC, 1-palmitoyl-2-oleoyl-L-α-phosphatidylcholine; $sPLA_2$, secretory phospholipase $A_2$.

10.1021/bi035982+ CCC: $27.50 
Published on Web 01/30/2004

Scheme 1: Conversion of Cholesterol to Cholest-4-en-3-one by Cholesterol Oxidase (COD)

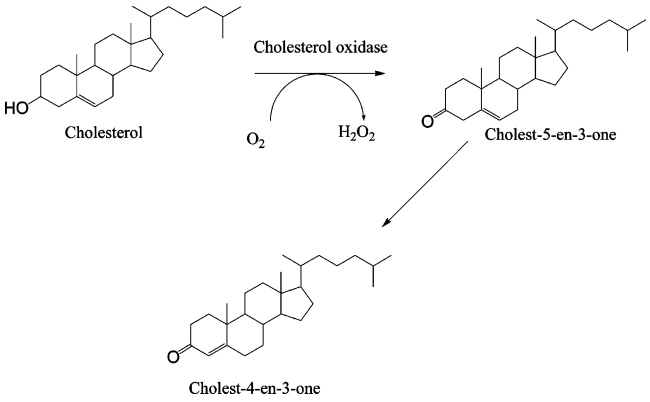


length of ~20 Å in the active site (*15*). This lid serves as a hydrophobic channel for extracting cholesterol from membrane bilayers to the active site of the enzyme, while the outer surface of the lid is hydrophilic (*18*). An extensive hydrogen-bonding network around a water molecule in the active site is required for the catalytic activity of COD (*19*−*21*).

The catalytic activity of COD is strongly affected by the environment of its substrate, cholesterol. Addition of detergents, such as sodium taurodeoxycholate and Triton X-100, drastically increases the extent and rate of COD-catalyzed cholesterol oxidation in a number of biological membranes as well as in lipid vesicles (*22*−*24*). The detergents disrupt the membrane, making all of the membrane cholesterol susceptible to the attack of COD. Phospholipase C (*22*, *23*) and sphingomyelinase (*25*) also promote membrane cholesterol oxidation by COD. These effects are caused by the removal of the steric blockage of cholesterol as a result of enzymatic cleavage of phospholipid polar headgroups. Because the activity of COD depends on its accessibility to membrane cholesterol, this enzyme has been used to probe cholesterol distribution in cells and cholesterol transbilayer asymmetry (*26*−*28*).

Membrane composition and lipid packing are also known to play an important role in the functionality of COD. Incorporation of diglyceride into the membrane increases sterol oxidation by COD (*29*). Further, the rate of cholesterol oxidation by COD is dependent upon the membrane cholesterol content (*29*) and the size of the phospholipid headgroup (*30*), and the first-order rate constant is increased with increasing membrane order as determined by diphenylhexatriene fluorescence anisotropy (*31*).

In recent years, we, as well as others, found evidence for regular patterns of sterol lateral distribution in a variety of phospholipid membranes (*32*−*41*; reviewed in ref *42*). According to the sterol regular distribution model (*32*), regularly distributed sterol superlattices and irregularly distributed lipid areas always coexist in sterol-containing membranes, with the ratio of regular to irregular regions reaching a local maximum at critical sterol mole fractions ($C_r$) (e.g., 15.4, 20.0, 22.2, 25.0, 33.3, 40.0, and 50.0 mol % sterol) (*38*, *43*). The model further proposes that sterol in the regular region is more accessible to the aqueous phase, due to tighter packing, than that in the irregular region (*32*, *36*, *37*). On the basis of these new findings in sterol lateral organization and the previous finding that the activity of COD depends on its accessibility to membrane cholesterol as mentioned earlier, we reasoned that the activity of COD should be regulated by membrane cholesterol content in an alternating manner showing a maximum at $C_r$.

In the present study, we obtained experimental evidence to support the above hypothesis. The effect of membrane sterol mole fraction on the initial rate of sterol oxidation by COD was investigated at 37 °C using large unilamellar vesicles (LUVs) composed of either cholesterol/1-palmitoyl-2-oleoyl-L-α-phosphatidylcholine (POPC) or dehydroergosterol (DHE)/POPC. During the sample preparation, the total sterol content in the membrane was fixed and the phosphatidylcholine (PC) content was varied, resulting in small cholesterol mole fraction increments (~0.1−0.3 mol % cholesterol). In the membrane systems examined, the initial catalytic activity of COD was found to change with sterol mole fraction in an alternating manner, and the activity exhibited a local maximum at $C_r$. The activity variation with cholesterol content was positively correlated to the regularly distributed area in the plane of the membrane as determined by nystatin fluorescence (*38*). We also determined the bimolecular acrylamide quenching rate constant $k_q$ of DHE fluorescence, in order to support the explanation that a maximal activity at $C_r$ resulted from sterol being more accessible to the aqueous phase (thus the enzyme). These results provide a new view on how COD is influenced by the physical environment of the bilayer substrate, which should be helpful for a more proper use of COD as a structural probe of membrane asymmetry and lateral organization. More importantly, the present work on COD, along with the previous study on phospholipase $A_2$ ($sPLA_2$) (*39*), suggests that the activities of some surface-acting enzymes may be regulated by the extent of sterol superlattice in the membrane in a substrate-dependent manner. When the substrate is a sterol, as it is with COD, the enzyme activity reaches a local maximum at $C_r$. When phospholipid is the substrate, the minimum enzyme activity is at $C_r$, as is the case with $sPLA_2$. Both phenomena appear to be in accordance with the sterol superlattice model.

## MATERIALS AND METHODS

*Materials*. POPC was purchased from Avanti Polar Lipids (Alabaster, AL). Cholesterol, cholest-4-en-3-one, nystatin, and dehydroergosterol (DHE) were purchased from Sigma (St. Louis, MO). COD was obtained from Calbiochem-Novabiochem (La Jolla, CA), and its concentration was determined as described (*44*) using bovine serum albumin as a standard. Cholesterol, DHE, and acrylamide were recrystallized from ethanol prior to use. The concentrations of DHE and nystatin were determined using their extinction coefficients: $\epsilon_{326nm,dioxane} = 10600\ M^{-1}\ cm^{-1}$ for DHE and $\epsilon_{304nm,methanol} = 74000\ M^{-1}\ cm^{-1}$ for nystatin.

*Preparation of Cholesterol/POPC Large Unilamellar Vesicles (LUVs).* Appropriate amounts of cholesterol and POPC were mixed in chloroform and then dried under nitrogen gas, followed by overnight lyophilization. The dried lipid mixtures were suspended in 0.1 M Tris buffer (pH 7.2, measured at room temperature, ~22 °C) containing 0.02% $NaN_3$. The dispersions were vortexed for 3 min at room temperature to make multilamellar vesicles (MLVs). The MLVs were cooled to −20 °C for 30 min and then incubated

Table 1: Comparison of Cholesterol Mole Percents in POPC Vesicles before (MLVs) and after (LUVs) the Extrusion[a]

| sample no. | [Chol], mM, MLVs | [PC], mM, MLVs | Chol, mol %, MLVs | [Chol], mM, LUVs | [PC], mM, LUVs | Chol, mol %, LUVs | Chol loss, % | PC loss, % | ΔChol, mol % |
|---|---|---|---|---|---|---|---|---|---|
| 1 | 1.25 | 4.00 | 23.8 | 1.05 | 3.39 | 23.6 | 16.0 | 15.2 | −0.2 |
| 2 | 1.25 | 3.93 | 24.1 | 1.05 | 3.29 | 24.2 | 16.0 | 16.3 | +0.1 |
| 3 | 1.25 | 3.85 | 24.5 | 1.06 | 3.27 | 24.5 | 15.2 | 15.1 | 0 |
| 4 | 1.25 | 3.79 | 24.8 | 1.08 | 3.29 | 24.7 | 13.6 | 13.2 | −0.1 |
| 5 | 1.25 | 3.75 | 25.0 | 1.11 | 3.30 | 25.2 | 11.2 | 12.0 | +0.2 |
| 6 | 1.25 | 3.69 | 25.3 | 1.10 | 3.23 | 25.4 | 12.0 | 12.5 | +0.1 |
| 7 | 1.25 | 3.65 | 25.5 | 1.12 | 3.26 | 25.6 | 10.4 | 10.7 | +0.1 |
| 8 | 1.25 | 3.58 | 25.9 | 1.06 | 3.05 | 25.8 | 15.2 | 14.8 | −0.1 |
| 9 | 1.25 | 3.52 | 26.2 | 1.04 | 2.90 | 26.4 | 16.8 | 17.6 | +0.2 |

[a] ΔChol = (Chol, mol %, LUV) − (Chol, mol %, MLV).

at room temperature for 30 min. This cooling−heating cycle was repeated three times to ensure an even distribution of lipids within each monolayer of the vesicles. The MLV samples were stored under nitrogen at room temperature for at least 4 days before extrusion. LUVs were prepared from MLVs using an extruder (Lipex Biomembranes Inc., Vancouver, British Columbia, Canada). The MLVs were extruded at room temperature 10−15 times through two stacked 800 nm Nucleopore polycarbonate filters (Costar) under nitrogen gas pressure. To avoid nonenzymatic oxidation of cholesterol, the LUV samples were stored under nitrogen at room temperature prior to activity, partitioning, and quenching measurements.

*Determinations of POPC and Cholesterol Mole Fractions in Cholesterol/POPC LUVs*. POPC and cholesterol concentrations of some LUVs were determined by the method of Bartlett (*45*) and Moore et al. (*22*), respectively. As illustrated in Table 1, the cholesterol mole percents in LUVs (after extrusion) and MLVs (before extrusion) differ very little (≤0.2 mol %), despite some loss of lipids during extrusion. Thus, for convenience, the sterol mole percents in MLVs before extrusion were used in assessing the relationship between sterol content and the activity of COD as well as other membrane parameters.

*Determination of COD Activity with Cholesterol/POPC LUVs as the Substrate.* The initial activity of *Streptomyces* COD was determined by following the time course of the absorbance at 240 nm due to the formation of the enzymatic oxidation product, cholest-4-en-3-one (*9*; reviewed in ref *10*). Appropriate amounts of LUVs with varying cholesterol mole percents were pipetted into cuvettes containing 50 mM sodium phosphate buffer (pH 7.0) so that each cuvette contained the same amount of cholesterol (238 nmol) with a fixed volume of solution (1 mL). COD (10 μL of 0.389 mg/mL) was then added into the sample cuvettes. Immediately after the addition, the absorbance at 240 nm was recorded over time on a Perkin-Elmer lambda-6 spectrophotometer (Shelton, CT). Light scattering from vesicles was corrected by using a reference cuvette containing identical lipid vesicles in the absence of the enzyme. Upon addition of COD, the absorbance changes virtually linearly with time in the first minute. The slope was taken as the initial oxidation rate of cholesterol by COD. This apparent initial activity, in terms of absorbance change at 240 nm/s, was then converted to the amount of cholest-4-en-3-one produced per second using a standard curve. The standard curve was constructed by measuring the maximal change of absorbance at 240 nm in the presence of varying amounts of standard cholest-4-en-3-one prepared by adding aliquots of 6 M authentic cholest-4-en-3-one in 2-propanol into 1.0 mL of 50 mM sodium phosphate buffer, pH 7.0. Each standard solution contained no more than 0.84% (v/v) 2-propanol, which has no effect on the absorbance at 240 nm. For all activity and standard curve measurements, the temperature of the sample was maintained at 37 ± 0.2 °C by a circulation bath, and Triton X-100 was not used.

Note that in the activity measurements we focused on the events taking place in the first minutes because only the initial events can be linked meaningfully to cholesterol regular distribution. After the reaction proceeds for a prolonged time, original lipid lateral organization may be perturbed by reaction products such as hydrogen peroxide and cholest-4-en-3-one.

*Determination of Regularly Distributed Lipid Area ($A_{reg}$) in Cholesterol/POPC LUVs.* The proportion of the membrane surface area where the sterol molecules are regularly distributed ($A_{reg}$) was determined as previously described (*38*). First, the partition coefficient of nystatin (*P*) from the aqueous phase to lipid vesicles was determined as a function of membrane cholesterol content in the ranges 18.7−21.3, 23.9−26.4, and 31.6−34.8 mol % cholesterol in POPC using the method of Wang et al. (*38*). This method took advantage of the fact that nystatin fluorescence intensity was enhanced when partitioning into lipid membranes and that the fluorescence enhancement was related to partition coefficient (*38*). Then, the nystatin partition coefficient was determined at low cholesterol concentrations (<5 mol %), where the cholesterol molecules were assumed to be virtually all irregularly distributed ($A_{reg} \sim 0$). At this low concentration region, the partition coefficient of nystatin was expected to increase linearly with increasing cholesterol concentration. By extrapolation, the partition coefficient of nystatin in the absence of regular distribution $P_0$(C) could be determined at any given cholesterol mole fraction C. We assumed that the packing of the lipid molecules is so perfect at the areas of regular distribution that there is no room for nystatin binding. We also assumed that, in the area of irregular region, the linear relationship is valid. With these assumptions, $A_{reg}$(C) was calculated near a given $C_r$ by the equation (*38*)

$$A_{reg}(C) = [P_0(C) - P(C)]/P_0(C_r).$$

*Determination of COD Activity with Dehydroergosterol/POPC LUVs as the Substrate.* Dehydroergosterol (DHE)/POPC LUVs were prepared in a way similar to cholesterol/POPC LUVs mentioned earlier, except that the temperature for vortexing, extrusion, and the heating side of the heating/cooling cycles was 37 °C, instead of room temperature.

Calculated amounts of DHE/POPC LUVs and 50 mM Tris-HCl buffer (pH 7.0) were added to a fluorescence cuvette. LUVs were then incubated for 15 min at 37 °C to bring each sample to thermal equilibrium. After incubation, time trace monitoring of DHE fluorescence intensity at 396 nm (8 nm band-pass) was begun using an excitation at 325 nm (0.5 nm band-pass) on an SLM 8000C fluorometer (Urbana, IL). After 60 s, 25 $\mu$L of 0.16 $\mu$mol/mL *Nocardia* sp. COD was added. The enzyme-to-substrate ratio was ~1:2000. The initial rate was calculated as fluorescence intensity change ($\Delta F$) per second for the first few minutes after addition of the enzyme. No significant photobleaching was noticed. The temperature of the sample in the fluorometer was controlled by a circulating bath, and the sample was stirred while fluorescence intensity was measured. Vesicle size was determined by photon correlation spectroscopy using the Malvern HS-1000 spectrometer (Worcs, U.K.); the light source was a He−Ne laser (633 nm), and the detection was made at an angle of 90° with respect to excitation. The possible presence of sterol microcrystals in the sample was checked by Rayleigh scattering using an SLM 8000C fluorometer with the excitation set at 500 nm (0.5 nm band-pass) and emission observed at 90° at 505 nm (8 nm band-pass).

*Acrylamide Quenching of DHE Fluorescence in DHE/Cholesterol/POPC LUVs.* The intensity of DHE fluorescence in DHE (fixed at 3 mol %)/cholesterol/POPC LUVs was measured as a function of acrylamide concentration at 37 °C using the SLM 8000C fluorometer. Vesicles were made in the same way as the cholesterol/POPC LUVs mentioned earlier. Samples were excited at 325 nm with a 1 nm band-pass. The emission was observed at 378 nm with an 8 nm band-pass. To calculate the quenching rate constant, the lifetime of DHE fluorescence in the same vesicles was measured in the absence of acrylamide at 37 °C using an ISS K2 phase-modulation fluorometer (ISS Inc., Champaign, IL). For DHE lifetime measurements, the light source we used was a He−Cd laser (Model 4240NB; LiConix Inc., Sunnyvale, CA) with excitation at 325 nm. The excitation polarizer was set at 35° with respect to the vertical plane. No emission polarizer was used. Phase and modulation values were determined relative to a *p*-bis[2-(5-phenyloxazolyl)]benzene (POPOP) reference solution (in ethanol), which has a lifetime of 1.35 ns at 325 nm excitation. DHE emission was observed through an Schott KV-389 filter. The lifetime was determined using modulation frequencies ranging from 70 to 200 MHz. The data were best fitted by a two-exponential decay law: $F(t) = \alpha_1 \exp(-t/\tau_1) + \alpha_2 \exp(-t/\tau_2)$, where $\alpha_i$ and $\tau_i$ are the preexponential factor and lifetime, respectively, for the $i$th exponent. The average lifetime $\langle\tau\rangle$ was calculated by the equation $\langle\tau\rangle = f_1\tau_1 + f_2\tau_2$ with $f_1 = \alpha_1\tau_1/(\alpha_1\tau_1 + \alpha_2\tau_2)$ and $f_2 = 1 - f_1$.

## RESULTS AND DISCUSSION

The effect of membrane cholesterol content on the initial activity of *Streptomyces* COD in cholesterol/POPC LUVs is presented in Figure 1. In the three concentration ranges (i.e., 18.8−21.2, 23.6−26.3, and 32.2−34.5 mol % cholesterol in POPC) examined, the initial catalytic activity of COD changed with membrane cholesterol content in an alternating manner, reaching a local maximum at 19.7, 25.0, and 33.4 mol % cholesterol. All of the samples examined here had the same amount of enzyme and substrate (cholesterol); the only difference was the sterol mole fraction. The result that a small change in sterol content (<1 mol %) caused a dramatic change in enzyme activity (3−5-fold) can only be attributed to a composition-dependent change in membrane organization, involving a large change in the accessibility of cholesterol to the COD. Within the experimental errors (~0.1−0.4 mol % sterol; *39*), the mole fraction values for maximal activity (designated as $C_a$) agreed with the critical cholesterol mole fractions (i.e., 20.0, 25.0, and 33.3 mol %, designated as $C_r$) theoretically predicted for maximal superlattice formation (*32*, *34*, *42*, *47*), giving a correlation coefficient, $r$, of 0.9999.

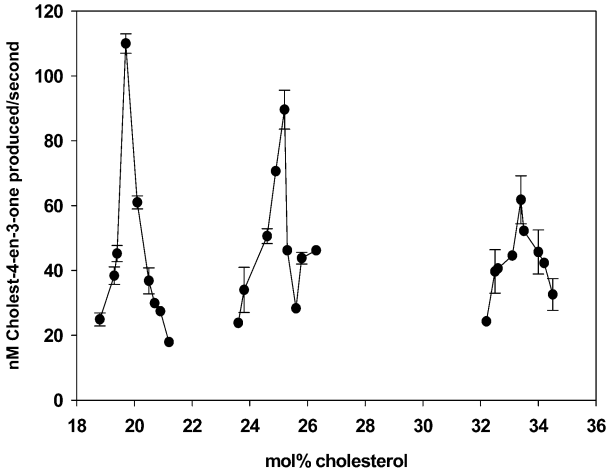


FIGURE 1: Effect of membrane cholesterol content on the initial rate of COD-catalyzed oxidation of cholesterol in cholesterol/POPC LUVs at 37 °C. The cholesterol concentration ranges examined are 18.8−21.2, 23.6−26.3, and 32.2−34.5 mol %. Vesicle size = ~800 nm in diameter. Vertical bars are the standard deviations calculated from three independently prepared samples.

To demonstrate that the alternating variation of COD activity with cholesterol content is related to the extent of sterol superlattice in the membrane, we have determined the regularly distributed surface areas, $A_{reg}$, of cholesterol/POPC LUVs in virtually the same cholesterol concentration regions (18.7−21.3, 23.9−26.4, and 31.6−34.8 mol % cholesterol in POPC). $A_{reg}$ was determined as described (*38*) with minor changes due to the use of unilamellar vesicles. In this approach, the partition coefficient ($P$) of nystatin in cholesterol/POPC LUVs was first determined fluorometrically as a function of membrane cholesterol content. In the cholesterol concentration ranges examined (18.7−21.3, 23.9−26.4, and 31.6−34.8 mol %), $P$ at 37 °C showed a biphasic change with cholesterol at 20.0, 24.8, and 33.4 mol % (Figure 2). These values are at or near the $C_r$ values theoretically predicted for maximal superlattice formation. The alternating pattern shown in Figure 2 agrees with the results obtained from MLVs (*38*), suggesting that the partitioning of the antifungal drug nystatin into lipid bilayers is regulated by the extent of sterol superlattice, regardless of vesicle type.

The $P$ values shown in Figure 2, combined with the nystatin partition coefficients into cholesteol/POPC LUVs in the absence of regular distribution as determined at low cholesterol mole fractions (≤5 mol %) ($P_0$, Figure 3A), allowed us to calculate (*38*) the proportion of the membrane surface area where the sterol molecules are regularly distributed ($A_{reg}$). As shown in Figure 3B, $A_{reg}$ varies with

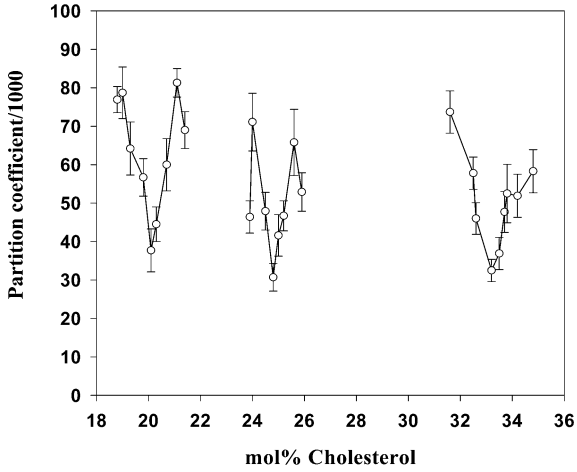


FIGURE 2: Cholesterol concentration dependence of the partition coefficient ($P$) of nystatin into cholesterol/POPC LUVs (~800 nm in diameter) at 37 °C. The cholesterol concentration ranges examined are 18.7−21.3, 23.9−26.4, and 31.6−34.8 mol %. Vertical bars are the errors of partition coefficients obtained from the parameter fitting procedure.

membrane cholesterol content in an alternating manner, showing a local maximum at 20.1, 24.8, and 33.2 mol % cholesterol, at which $A_{reg}$ is 0.849, 0.886, and 0.911, respectively. These mole fractions (designated as $C_p$) are correlated well with the mole fractions of activity maxima ($C_a$) obtained from Figure 1, giving a correlation coefficient of 0.9995. Taken together, a good correlation of $C_a$ with the theoretically predicted $C_r$ as well as the semiexperimentally determined $C_p$ lends strong support that the activity of COD in membrane bilayers is regulated by the extent of cholesterol superlattice in the plane of the membrane.

In Figure 1 the activity maxima at $C_a$ are decreasing with increasing sterol mole fraction, while in Figure 3B the maxima of $A_{reg}$ at $C_p$ are increasing slightly with increasing sterol mole fraction. This difference is probably due to the rather large error of $A_{reg}$ (Figure 3B); thus, it is possible that a trend similar to the one in Figure 1 is within the error limit of the data shown in Figure 3B. Another plausible explanation is the following. The pattern of lipid regular distribution varies with $C_r$ (*32*, *42*, *47*−*50*), and different regular distribution patterns may result in different substrate accessibility to COD. Hence, although the activity of COD in membrane bilayers is regulated by the extent of sterol superlattice in the neighborhood of a critical mole fraction as mentioned earlier, membranes with the same extent of sterol superlattice (i.e., the same $A_{reg}$ value), but with lipid compositions at different critical sterol mole fraction regions, do not necessarily have the same COD activity.

Dehydroergosterol (DHE) behaves similarly to cholesterol and ergosterol in terms of sterol superlattice formation (*36*, *37*). Thus, if the activity of COD in membrane bilayers is regulated by the extent of sterol superlattice as mentioned earlier, the alternating variation of activity with sterol content should occur not only in cholesterol/POPC LUVs but also in DHE/POPC vesicles. DHE has three conjugated double bonds in the steroid ring and nine carbons including one double bond in the side chain, whereas cholesterol has one double bond in the ring and eight carbons with no double bonds in the side chain. However, according to previous COD studies on other sterols (*10*, *51*), these structural

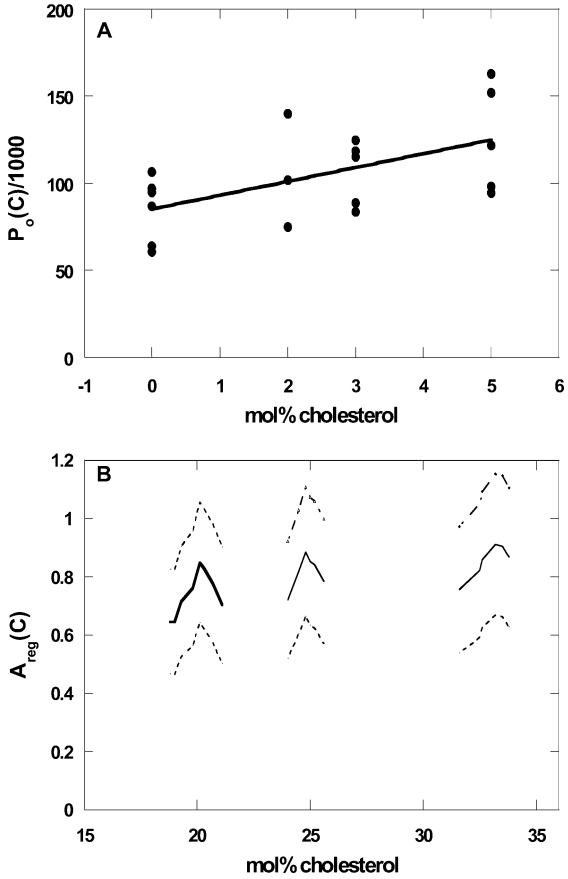


FIGURE 3: Estimation of regularly distributed areas in cholesterol/POPC LUVs (~800 nm in diameter). (A) Cholesterol concentration dependence of the partition coefficient of nystatin into cholesterol/POPC LUVs in the cholesterol concentration range of 0−5 mol % at 37 °C. The solid line is the linear regression of experimental points (dark circles). (B) Area of regular distribution relative to the total outermost membrane surface ($A_{reg}$) plotted against cholesterol content in cholesterol/POPC LUVs at 37 °C. The solid lines are the expected values of $A_{reg}$; the dotted lines are the standard deviations from the expected values of $A_{reg}$.

differences are relatively small, and COD should be active toward both cholesterol and DHE. We believe that COD oxidizes the hydroxyl group of DHE and then isomerizes the conjugated double bond system of DHE, in a way similar to the oxidation of cholesterol, leading to a decrease in DHE fluorescence intensity. Indeed, upon addition of COD, the fluorescence intensity of DHE in DHE/POPC LUVs decreased over time (Figure 4A). This decay curve, which represents a new fluorescence assay for COD, allowed us to determine the initial rate of COD-catalyzed sterol oxidation in DHE/POPC LUVs. As shown in Figure 4B, a biphasic change in initial rate of DHE oxidation appears at 19.7 mol %. This mole percent is close to the theoretical value of 20.0 mol % predicted for maximal superlattice formation in the sterol concentration range (18.8−21.2 mol % sterol) examined. Taken together, the results in Figures 4 and 1 suggest that the activity of COD in membrane bilayers is regulated by the extent of sterol superlattice, irrespective of sterol type and for varying vesicle sizes [from ~168 nm (Figure 4) to ~800 nm (Figure 1)], a result consistent with the properties of lipid regular distribution previously characterized (*37*, *52*).

The activity maxima at $C_r$ cannot be attributed to the presence of sterol microcrystals for two reasons. First, sterol crystals usually occur above 67 mol % in phosphatidylcholine

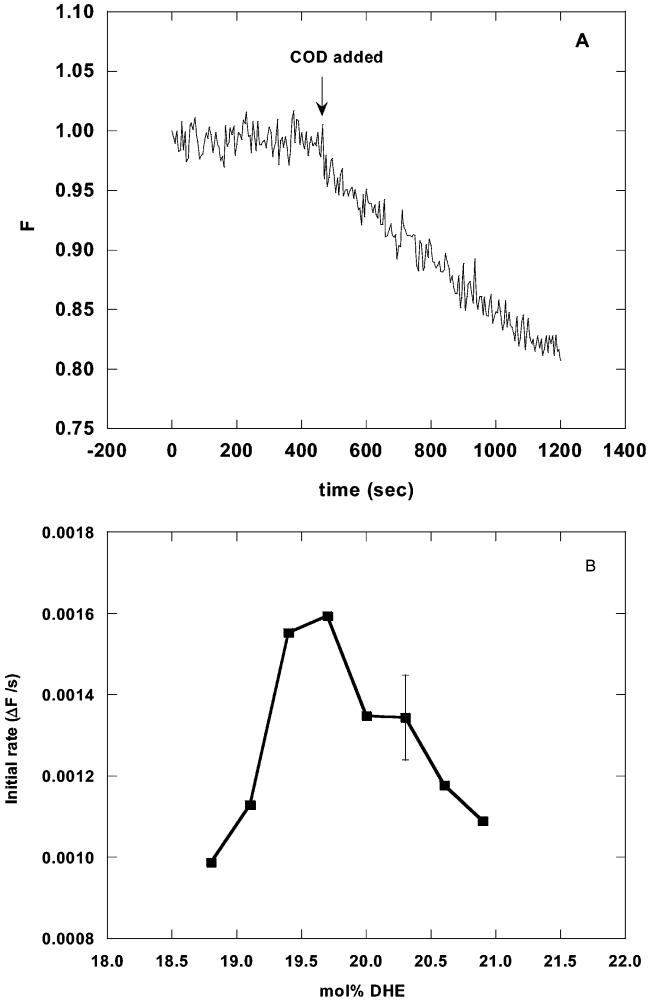


FIGURE 4: (A) Illustration of the new fluorescence assay of COD activity using DHE as the substrate. *F* is the relative fluorescence intensity of DHE in 20.9 mol % DHE/POPC LUVs. (B) Effect of membrane DHE content on the initial rate (expressed as the fluorescence intensity change, Δ*F*, per second) of COD-catalyzed sterol oxidation in DHE/POPC LUVs. The vertical bar is the standard deviation calculated from three independently prepared samples. For both (A) and (B), temperature = 37 °C and vesicle size = ∼168 nm in diameter.

bilayers (*53*, *54*); this mole fraction is much higher than those used in the present study. Second, we did not detect any significant change of Raleigh light scattering with membrane sterol content in sterol/POPC LUVs over the sterol concentration range examined (data not shown).

The results shown in Figures 1 and 4 provide the second example, in addition to the secretory phospholipase $A_2$ (sPLA$_2$) (*39*), that the activity of a membrane surface-acting enzyme varies with membrane sterol content in an alternating manner according to the extent of cholesterol superlattice. However, in contrast to sPLA$_2$, which exhibits an activity minimum at $C_r$ (*39*), COD displays an activity maximum at those critical concentrations. This difference can be understood as follows.

sPLA$_2$ acts favorably with phospholipid bilayers containing membrane defects (ref *6* and references cited therein). Our previous experimental data showed that membrane defects change with sterol content in an alternating manner, showing a minimum at $C_r$ (*32*, *35*, *37*, *52*). Computer simulations also showed that the relative size of the irregular region reaches a local minimum at $C_r$ (*43*). According to the lipid regular

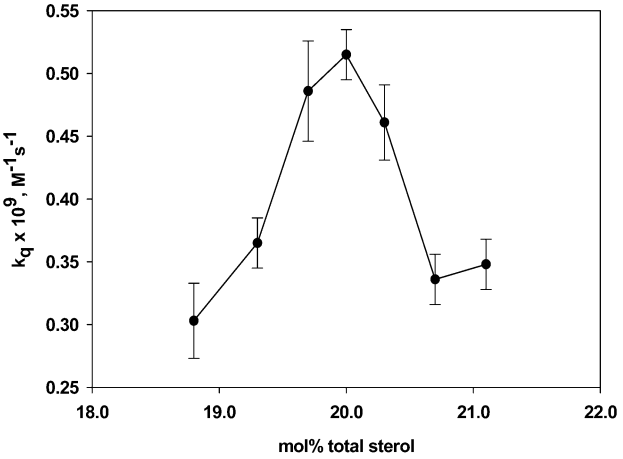


FIGURE 5: Total sterol concentration dependence of the bimolecular acrylamide quenching rate constant of DHE fluorescence $k_q$ in 3 mol % DHE/cholesterol/POPC LUVs at 37 °C. Vesicle size = ∼800 nm in diameter. Vertical bars are the standard deviations calculated from three independently prepared samples.

distribution model, membrane defects are allowed only in the irregular region, not in the regular region (*43*, *52*). Thus, the sterol regular distribution model can explain why the hydrolytic activity of sPLA$_2$ exhibits a local minimum at $C_r$ (*39*).

The catalytic activity of COD is strongly dependent upon its accessibility to the substrate (membrane sterol), as mentioned earlier. According to the regular distribution model, sterol in the regular region is more accessible to aqueous phase, due to tighter packing, than sterol in the irregular region, and the ratio of regular to irregular region reaches a maximum at $C_r$ (*32*, *36*, *42*). Hence, the sterol regular distribution model can also explain why the activity of COD reaches a local maximum at $C_a$ (Figures 1 and 4).

The assertion that sterol in the regular region is more accessible to the aqueous phase than sterol in the irregular region was originally based on the finding of DHE fluorescence intensity dips at $C_r$ in DHE/dimyristoyl-L-α-phosphatidylcholine (DMPC) MLVs (*32*). This assertion was subsequently supported by an acrylamide quenching study, which showed that the bimolecular rate constant of acrylamide quenching of DHE fluorescence exhibited peaks at $C_r$ in DHE/DMPC MLVs (*36*). However, previous studies were made on DMPC MLVs. To provide evidence that sterol becomes more accessible to the aqueous phase at $C_r$ in a membrane system structurally comparable to that used in the present activity measurement, we have conducted an acrylamide quenching study on DHE/cholesterol/POPC LUVs (∼800 nm in diameter) (Figure 5). In this experiment, the acrylamide quenching of DHE fluorescence intensity was monitored as a function of total membrane sterol content, which equals the mole percent of cholesterol plus the mole percent of DHE (fixed at 3 mol %). Using the average lifetime $\tau_0$ measured in the absence of acrylamide and assuming a dynamic quenching mechanism, the bimolecular quenching rate constant $k_q$ was calculated. As shown in Figure 5, $k_q$ varies with total sterol content in a biphasic manner, exhibiting a peak value at 20.0 mol % total sterol. This value is the critical sterol mole fraction predicted for maximal superlattice formation in the concentration range examined (18.8−21.1 mol %). $k_q$ is a parameter reflecting how frequently the water-soluble acrylamide collides with

the membrane DHE. Thus, the quenching data (Figure 5) support the idea that, in DHE/cholesterol/POPC LUVs, sterols at $C_r$ are more accessible to the aqueous phase than sterols at non-$C_r$. This property may arise from two possibilities (*36*, *42*). First, in the regular regions, sterol is embedded less deeply than in the irregular regions. Second, sterol in the regular regions is less shielded from water by the neighboring phospholipid polar headgroups than in the irregular regions. It is likely that the polar headgroup in the regular and irregular regions adopts a different conformation. In either case, sterols should become more exposed to the aqueous phase (thus the COD) at $C_r$. As a result, at $C_r$, sterols are more easily taken up to the active site via the lid of the COD (mentioned earlier) and, hence, more readily oxidized.

The alternating variation of COD activity with sterol content is a new finding probably because previous studies of COD in membrane bilayers did not use small sterol mole fraction increments or did not pay much attention to membrane lateral organization stability. Sonicated vesicles have considerable curvature stress, which would attenuate superlattice formation (*52*). Vesicles without sufficient incubation time and careful thermal history control may not reveal evidence for superlattice formation (*42*).

The observation of a COD activity maximum and water accessibility maximum at $C_r$ implies that the umbrella effect caused by the phospholipid polar headgroups to protect cholesterol from being exposed to water was not the same for all sterol mole fractions. This finding was not predicted by the umbrella model proposed by Huang and Feigenson (*53*) but is consistent with their finding that cholesterol begins to precipitate out of phospholipid bilayers at certain high critical sterol mole fractions for superlattice formation (*50*). It is likely that the overall umbrella effect of the polar headgroup for covering cholesterol is weakened at $C_r$ where the acyl chain packing reaches an optimum (*35*, *37*, *52*). The $C_a$ values for maximal COD activity (Figures 1 and 4) may coincide with the stoichiometries due to the formation of sterol/phospholipid complexes (*55*, *56*). Future work will be required to evaluate how the complex formation theory would explain the opposite alternating behavior of $sPLA_2$ and COD activity with sterol content.

Our present data may provide a new interpretation for why two kinetic pools were observed for cholesterol oxidation by COD in the outermost layer of the cell plasma membrane. For example, a slow rate (0.2%/min) and a fast initial rate of cholesterol oxidation (>1.2%/min) were observed in rabbit intestinal brush border membrane (*57*). The slow phase was proposed to originate from cholesterol associated with membrane protein and the fast phase from membrane cholesterol not associated with membrane proteins (*57*). Similar differential kinetic pools were observed in other cell membranes, and the results were often ascribed to cholesterol-rich and cholesterol-poor lipid domains in the membrane (*22*, *23*, *27*, *28*, *58*, *59*). Our present data, however, suggest that those kinetic pools may have originated from cholesterol in the regular and irregular regions.

More importantly, the present work on COD, along with the previous study on phospholipase $A_2$ (*39*), suggests that the activities of some surface-acting enzymes may be regulated by the extent of sterol superlattice in the membrane in a substrate-dependent manner. When the substrate is a sterol, as it is with COD, the enzyme activity reaches a local maximum at $C_r$. When phospholipid is the substrate, the enzyme activity is minimum at $C_r$, as is the case with $sPLA_2$. Both phenomena appear to be in accordance with the sterol superlattice model and manifest the functional importance of membrane cholesterol content. Other surface-acting enzymes, such as phospholipase C and sphingomyelinase, may also follow this pattern; many of these enzymes play pivotal roles in metabolism and signal transduction. In the future, it would be of great interest to further investigate how those surface-acting enzymes and their associated cellular activities are affected by the extent of sterol superlattice in the membrane.

## REFERENCES


1. Capper, E. A., and Marshall, L. A. (2001) Mammalian phospholipases A(2): mediators of inflammation, proliferation and apoptosis, *Prog. Lipid Res. 40*, 167−197.
2. Kudo, I., and Murakami, M. (2002) Phospholipase A2 enzymes, *Prostaglandins Other Lipid Mediat. 68*−*69*, 3−58.
3. Taketo, M. M., and Sonoshita, M. (2002) Phospolipase A2 and apoptosis, *Biochim. Biophys. Acta 1585*, 72−76.
4. Balsinde, J., Winstead, M. V., and Dennis, E. A. (2002) Phospholipase A(2) regulation of arachidonic acid mobilization, *FEBS Lett. 531*, 2−6.
5. Goni, F. M., and Alonso, A. (2002) Sphingomyelinases: enzymology and membrane activity, *FEBS Lett. 531*, 38−46.
6. Honger, T., Jorgensen, K., Biltonen, R. L., and Mouritsen, O. G. (1996) Systematic relationship between phospholipase A2 activity and dynamic lipid bilayer microheterogeneity, *Biochemistry 35*, 9003−9006.
7. Harris, F. M., Smith, S. K., and Bell, J. D. (2001) Physical properties of erythrocyte ghosts that determine susceptibility to secretory phospholipase $A_2$, *J. Biol. Chem. 276*, 22722−22731.
8. Sugar, I. P., Mizuno, N. K., Momsen, M. M., and Brockman, H. L. (2001) Lipid lateral organization in fluid interfaces controls the rate of colipase association, *Biophys. J. 81*, 3387−3397.
9. Smith, A. G., and Brooks, C. J. W. (1977) The substrate specificity and stereochemistry, reversibility and inhibition of the 3-oxo steroid $\Delta^4$-$\Delta^5$-isomerase component of cholesterol oxidase, *Biochem. J. 167*, 121−129.
10. MacLachlan, J., Wotherspoon, A. T. L., Ansell, R. O., and Brooks, C. J. W. (2000) Cholesterol oxidase: sources, physical properties and analytical applications, *J. Steroid Biochem. Mol. Biol. 72*, 169−195.
11. Murooka, Y., Ishizaki, T., Nimi, O., and Maekawa, N. (1986) Cloning and expression of a *Streptomyces* cholesterol oxidase gene in *Streptomyces lividans* with plasmid pIJ702, *Appl. Environ. Microbiol. 52*, 1382−1385.
12. Ishizaki, T., Hirayama, N., Shinkawa, H., Nimi, O., and Murooka, Y. (1989) Nucleotide sequence of the gene for cholesterol oxidase from a *Streptomyces* sp., *J. Bacteriol. 171*, 596−601.
13. Ohta, T., Fujishiro, K., Yamaguchi, K., Tamura, Y., Aisaka, K., Uwajima, T., and Hasegawa, M. (1991) Sequence of gene *choB* encoding cholesterol oxidase of *Brevibacterum sterolicum*: comparison with *choA* of *Streptomyces* sp. SA-COO, *Gene 103*, 93−96.
14. Vrielink, A., Lloyd, L. F., and Blow, D. M. (1991) Crystal structure of cholesterol oxidase from *Brevibacterum sterolicum* refined at 1.8 Å resolution, *J. Mol. Biol. 219*, 533−554.
15. Li, J., Vrielink, A., Brick, P., and Blow, D. M. (1993) Crystal structure of cholesterol oxidase complexed with a steroid substrate: implications for flavin adenine dinucleotide dependent alcohol oxidase, *Biochemistry 32*, 11505−11515.
16. Yue, Q. K., Kass, I. J., Sampson, N. S., and Vrielink, A. (1999) Crystal structure determination of cholesterol oxidase from *Streptomyces* and structural characterization of key active site mutants, *Biochemistry 38*, 4277−4286.
17. Ghoshroy, K. B., Zhu, W., and Sampson, N. S. (1997) Investigation of membrane disruption in the reaction catalyzed by cholesterol oxidase, *Biochemistry 36*, 6133−6140.
18. Sampson, N. S., Kass, I. J., and Ghoshroy, K. B. (1998) Assessment of the role of an Ω loop cholesterol oxidase: a truncated loop mutant has altered substrate specificity, *Biochemistry 37*, 5770−5778.

19. Nishiya, Y., Harada, N., Teshima, S. I., Yamashita, M., Fujii, I., Hirayama, N., and Murooka, Y. (1997) Improvement of thermal stability of Streptomyces cholesterol oxidase by random mutagenesis and a structural interpretation, *Protein Eng. 10*, 231−235.
20. Kass, I. J., and Sampson, N. S. (1998) Evaluation of the role of $His^{447}$ in the reaction catalyzed by cholesterol oxidase, *Biochemistry 37*, 17990−18000.
21. Yamashita, M., Toyama, M., Ono, H., Fujii, I., Hirayama, N., and Murooka, Y. (1998) Separation of the two reactions, oxidation and isomerization, catalyzed by *Streptomyces* cholesterol oxidase, *Protein Eng. 11*, 1075−1081.
22. Moore, N. F., Patzer, E. J., Barenholz, Y., and Wagner, R. R. (1977) Effect of phospholipase C and cholesterol oxidase on membrane integrity, microviscosity, and infectivity of vesicular stomatitis virus, *Biochemistry 16*, 4708−4715.
23. Patzer, E. J., Wagner, R. R., and Barenholz, Y. (1978) Cholesterol oxidase as a probe for studying membrane organization, *Nature 274*, 394−395.
24. Thurnhofer, H., Gains, N., Mutsch, B., and Hauser, H. (1986) Cholesterol oxidase as a structural probe of biological membranes: its application to brush-border membrane, *Biochim. Biophys. Acta 856*, 174−181.
25. Slotte, J. P. (1992) Enzyme-catalyzed oxidation of cholesterol in pure monolayers at the air/water interface, *Biochim. Biophys. Acta 1123*, 326−333.
26. Backer, J. M., and Dawidowicz, E. A. (1981) Transmembrane movement of cholesterol in small unilamellar vesicles detected by cholesterol oxidase, *J. Biol. Chem. 256*, 586−588.
27. Lange, Y. (1992) Tracking cell cholesterol with cholesterol oxidase, *J. Lipid Res. 33*, 315−321.
28. Boesze-Battaglia, K., Clayton, S. T., and Schimmel, R. J. (1996) Cholesterol redistribution within human platelet plasma membrane: evidence for a stimulus-dependent event, *Biochemistry 35*, 6664−6673.
29. De Martinez, S., and Green, C. (1979) The action of cholesterol oxidases on cholesterol in vesicles and micelles, *Biochem. Soc. Trans. 7*, 978−979.
30. Pal, R., Barenholz, Y., and Wagner, R. R. (1980) Effect of cholesterol concentration on organization of viral and vesicle membranes, *J. Biol. Chem. 226*, 5802−5806.
31. Crockett, E. L., and Hazel, J. R. (1995) Sensitive assay for cholesterol in biological membranes reveals membrane-specific differences in kinetics of cholesterol oxidase, *J. Exp. Zool. 271*, 190−195.
32. Chong, P. L.-G. (1994) Evidence for regular distribution of sterols in liquid crystalline phosphatidylcholine bilayers, *Proc. Natl. Acad. Sci. U.S.A. 91*, 10969−10073.
33. Parasassi, T., Giusti, A. M., Raimondi, M., and Gratton, E. (1995) Abrupt modifications of phospholipid bilayer properties at critical cholesterol concentrations, *Biophys. J. 68*, 1895−1902.
34. Virtanen, J. A., Ruonala, M., Vauhkonen, M., and Someharju, P. (1995) Lateral organization of liquid-crystalline cholesterol-dimyristoylphosphatidylcholine bilayers. Evidence for domains with hexagonal and centered rectangular cholesterol superlattices, *Biochemistry 34*, 11568−11581.
35. Chong, P. L.-G. (1996) Membrane-free volume variation with bulky lipid concentration by regular distribution: A functionally important membrane property explored by pressure studies of phosphatidylcholine bilayers, in *High-Pressure Effects in Molecular Biophysics and Enzymology* (Markley, J. L., Northrop, D. B., and Royer, C. A., Eds.) pp 298−313, Oxford University Press, New York.
36. Chong, P. L.-G., Liu, F., Wang, M. M., Truong, K., Sugar, I. P., and Brown, R. E. (1996) Fluorescence evidence for cholesterol regular distribution in phosphatidylcholine and in sphingomyelin lipid bilayers, *J. Fluoresc. 6*, 221−230.
37. Liu, F., Sugar, I. P., and Chong, P. L.-G. (1997) Cholesterol and ergosterol superlattices in three-component lipid crystalline lipid bilayers as revealed by dehydroergosterol fluorescence, *Biophys. J. 72*, 2243−2254.
38. Wang, M. M., Sugar, I. P., and Chong, P. L.-G. (1998) Role of the sterol superlattice in the partitioning of the antifungal drug nystatin into lipid membranes, *Biochemistry 37*, 11797−11805.
39. Liu, F., and Chong, P. L.-G. (1999) Evidence for a regulatory role of cholesterol superlattices in the hydrolytic activity of secretory phospholipase A2 in lipid membranes, *Biochemistry 38*, 3867−3873.
40. Wang, M. M., Sugar, I. P., and Chong, P. L.-G. (2002) Effect of double bond position on dehydroergosterol fluorescence intensity dips in phosphatidylcholine bilayers with saturated *sn*-1 and monoenoic *sn*-2 acyl chains, *J. Phys. Chem. 106*, 6338−6345.
41. Cannon, B., Heath, G., Huang, J., Somerharju, P., Virtanen, J. A., and Cheng, K. H. (2003) Time-resolved fluorescence and Fourier transform infrared spectroscopic investigations of lateral packing defects and superlattice domains in compositionally uniform cholesterol/phosphatidylcholine bilayers, *Biophys. J. 84*, 3777−3791.
42. Chong, P. L.-G., and Sugar, I. P. (2002) Fluorescence studies of lipid regular distribution in membranes, *Chem. Phys. Lipids 116*, 153−175.
43. Sugar, I. P., Tang, D., and Chong, P. L.-G. (1994) Monte Carlo simulation of lateral distribution of molecules in a two-component lipid membrane. Effect of long-range repulsive interactions, *J. Phys. Chem. 98*, 7201−7210.
44. Lowry, O. H., Rosbrough, N. J., Farr, A. L., and Randall, R. J. (1951) Protein measurement with the Folin phenol reagent, *J. Biol. Chem. 193*, 265−275.
45. Bartlett, G. R. (1959) Phosphorus assay in column chromatography, *J. Biol. Chem. 234*, 466−468.
46. Virtanen, J. A., Ruonala, M., Vauhkonen, M., and Somerharju, P. (1995) Lateral organization of liquid-crystalline cholesterol-dimyristoylphosphatidylcholine bilayers. Evidence for domains with hexagonal and centered rectangular cholesterol superlattices, *Biochemistry 34*, 11568−11581.
47. Somerharju, P. J., Virtanen, J. A., and Cheng, K. H. (1999) Lateral organization of membrane lipids. The superlattice view, *Biochim. Biophys. Acta 1440*, 32−48.
48. Virtanen, J. A., Somerharju, P., and Kinnunen, P. K. J. (1988) Prediction of patterns for the regular distribution of soluted guest molecules in liquid crystalline phospholipid membranes, *J. Mol. Electron. 4*, 233−236.
49. Tang, D., and Chong, P. L.-G. (1992) E/M dips: evidence for lipids regularly distributed into hexagonal super-lattices in pyrene-PC/DMPC binary mixtures at specific concentrations, *Biophys. J. 63*, 903−910.
50. Huang, J. (2002) Exploration of molecular interactions in cholesterol superlattices: Effect of multibody interactions, *Biophys. J. 83*, 1014−1025.
51. Slotte, J. P., Jungner, M., Vilcheze, C., and Bittman, R. (1994) Effect of sterol side-chain structure on sterol phosphatidylcholine interactions in monolayers and small unilamellar vesicles, *Biochim. Biophys. Acta 1190*, 435−443.
52. Chong, P. L.-G., Tang, D., and Sugar, I. P. (1994) Exploration of physical principles underlying lipid regular distribution: effects of pressure, temperature, and radius of curvature on E/M dips in pyrene-labeled PC/DMPC binary mixtures, *Biophys. J*. 66, 2029−2038.
53. Huang, J., and Feigenson, G. W. (1999) A microscopic interaction model of maximum solubility of cholesterol in lipid bilayers, *Biophys. J. 76*, 2142−2157.
54. Huang, J., Buboltz, J. T., and Feigenson, G. W. (1999) Maximum solubility of cholesterol in phosphatidylcholine and phosphatidylethanolamine bilayers, *Biochim. Biophys. Acta 1417*, 89−100.
55. Radhakrishnan, A., and McConnell, H. M. (1999) Cholesterol-phospholipid complexes in membranes, *J. Am. Chem. Soc. 121*, 486-487.
56. McConnell, H. M., and Vrljic, M. (2003) Liquid−liquid immiscibility in membranes, *Annu. Rev. Biophys. Biomol. Struct. 32*, 469−492.
57. Bloj, B., and Zilversmit, D. B. (1982) Heterogeneity of rabbit intestine brush border plasma membrane cholesterol, *J. Biol. Chem. 257*, 7608−7614.
58. Hale, J. E., and Schroeder, F. (1982) Asymmetric transbilayer distribution of sterol across plasma membranes determined by fluorescence quenching of dehydroergosterol, *Eur. J. Biochem. 122*, 649−661.
59. Yandouzi, E. H. E., and Le Grimellec, C. (1993) Effect of cholesterol oxidase treatment on physical state of renal brush border membranes: evidence for a cholesterol pool interacting weakly with membrane lipids, *Biochemistry 32*, 2047−2052.


BI035982+